Supporting Information

Enhancing Nitrogen Electroreduction to Ammonia by Doping Chlorine on Reduced Graphene Oxide

Peng Huang[†,1], *Zhuo Cheng*[‡,1,*], *Liang Zeng*[§], *Jian Yu*[†], *Lulu Tan*[†], *Pinak Mohapatra*[‡], *Liang-Shih Fan*[‡,] *and Yujie Zhu*[†,|,*]

[†] School of Chemistry, Beihang University, Beijing 100191, P. R. China

[‡] William G. Lowrie Department of Chemical and Biomolecular Engineering, 151 West Woodruff Avenue, The Ohio State University, Columbus, OH 43210, United States

[§] Key Laboratory for Green Chemical Technology of Ministry of Education, School of Chemical Engineering and Technology, Collaborative Innovation Center of Chemical Science and Engineering, Tianjin University, Tianjin 300072, P. R. China

[|] Beijing Advanced Innovation Center for Biomedical Engineering, Beihang University, Beijing 100191, P. R. China

*Corresponding authors. Email: cheng.963@osu.edu (Z. C.), yujiezhu@buaa.edu.cn (Y. Z.)

[1] These authors make equal contributions to this work.

Chemicals and Materials: Sulfuric acid (H_2SO_4, Beijing Chemical Works, 95%~98%), L-ascorbic acid ($C_6H_8O_6$, XiLong scientific, ≥99.7%), potassium chloride (KCl, Beijing Chemical Works, ≥99.5%), ammonium chloride (NH_4Cl, Alfa Aesar, ≥99.5%), hydrazine hydrate ($N_2H_4 \cdot H_2O$, Xiya reagent, 80%), sodium hydroxide (NaOH, Alfa Aesar, 98%), salicylic acid ($C_7H_6O_3$, Alfa Aesar, 99%), trisodium citrate dihydrate ($Na_3C_6H_5O_7 \cdot 2H_2O$, Alfa Aesar, 99%), sodium nitroferricyanide dihydrate ($Na_2Fe(CN)_5NO \cdot 2H_2O$, Alfa Aesar, 99%), sodium hypochlorite solution (NaClO, Alfa Aesar, available chlorine 11%~14%), para-(dimethylamino) benzaldehyde (p-$C_9H_{11}NO$, Innochem, 99%), hydrochloric acid (HCl, Beijing Chemical Works, 36%~38%), ethyl alcohol (C_2H_5OH, Beijing Chemical Works, ≥99.8%), carbon paper (Toray, TGP-H-060), Nafion D-521 dispersion (Dupont, 5% W/W), Nafion membrane (Dupont, 117), deionized water (Millipore), N_2 gas (99.999%), and Ar gas (99.999%). All chemical reagents were used as received without further purification.

Syntheses of the Cl-doped Reduced Graphene Oxide (Cl-RGO): The reduction of graphene oxide (GO) was performed in an aqueous solution by using L-ascorbic acid at ambient conditions. Here, L-ascorbic acid instead of hydrazine hydrate was employed as the reducing agent to avoid introducing unnecessary nitrogen sources. Typically, 400 mg of L-ascorbic acid was added to 50 mL of 0.4 mg mL^{-1} GO aqueous dispersion under vigorous stirring. After stirred for two days, the solution was centrifuged to obtain the precipitate, which was thoroughly washed with deionized water for several times and then freeze-dried for two days to obtain the reduced graphene oxide (RGO). Subsequently, 2 mg of RGO was added into 15 mL of H_2SO_4 (10 mol L^{-1}) and ultrasonically dispersed for 60 min. After that, 10 ml of NaClO (0.5 mol L^{-1}) solution was poured into the above acid solution with caution, which was kept stirring at ambient conditions for 10 h in a fume hood. Finally, the solution was centrifuged to obtain the precipitate, which was then washed with water and ethanol for several times, and subsequently dried in a vacuum oven set at 40 °C to obtain the Cl-RGO.[1-4]

Characterizations: The surface morphology of all samples were observed on a Quanta

250 FEG environmental scanning electron microscope (SEM). Wide-angle X-ray diffraction (XRD) patterns were recorded on a Shimadzu XRD-6000 powder diffractometer equipped with a Cu Kα source (λ=0.154). X-ray photoelectron spectroscopy (XPS) studies were conducted on a Thermo Scientific Escalab 250Xi. The binding energies obtained in the XPS spectral analysis were calibrated by C1s = 284.8 eV. Transmission electron microscopy (TEM) images and TEM-mapping images were performed by Tecnai G2 F20 S-TWIN operating at an acceleration voltage of 200 kV. Fourier transformed infrared spectroscopy (FTIR) was taken to investigate the different bonding present in the samples with wavenumber ranging from 400 to 3500 cm^{-1} on Nicolet iN10MX. Raman spectra of the samples were collected on a LabRAM HR800.

Electrochemical Testing: Before electrochemical tests, the carbon paper (1cm×2cm) was sonicated for 30 min in a mixture of acetone, isopropanol, and water with a volume ratio of 1:1:1. Afterward, it was washed with DI water for three times and dried at 70 °C in vacuum. The Nafion 117 membrane was sequentially pretreated in H_2O_2 (10%) aqueous solution, H_2SO_4 (0.5 M), and DI water at 70 °C for one hour each, respectively. A three-electrode airtight electrochemical H-type cell configuration with two compartments which were separated by the Nafion 117 membrane was used for all electrochemical tests. For the preparation of the working electrodes, 2 mg of the sample was dispersed in 2 mL of the aqueous solution containing 1.8 mL ethanol and 0.2 mL Nafion. The mixture was sonicated for at least 30 min to obtain a uniform ink. Then, 80 μL of ink was drop cast onto the carbon paper (sample loading: 40 μg cm^{-2}), which was then dried at 55 °C in an oven for two minutes to serve as the working electrode (immersed area: 1 cm^2). In addition, platinum gauze electrode (1cm×1cm) and Ag/AgCl electrode (saturated KCl) were used as the counter electrode and reference electrode, respectively. All potentials reported in this work were referred to the RHE by adding a value of (0.197 + 0.0591 pH) V. Before the NRR measurements, ultra-high purity N_2 was pre-purified in advance through a gas-washing cell, and then bubbled into the cathode chamber containing 0.05 M H_2SO_4 for 30 minutes under magnetic stir. Afterward, potentiostatic tests were carried out with N_2 continuously fed into the

cathodic compartment. All electrochemical experiments were conducted on a computer-controlled CHI 660E electrochemical workstation. All the NRR tests were repeated three times to ensure the reliability of the data.

Quantification of Ammonia：

1. Preparation of indophenol blue reagent

(1) Chromogenic reagent: 8.2 g NaOH, 11.7 g salicylic acid, and 13.4 g trisodium citrate dihydrate were dissolved in 200 mL of DI water.

(2) Oxidizing solution: 2.37 mL of NaClO was dissolved in 100 mL of DI water.

(3) Catalyzing reagent: 1.03 g of sodium nitroferricyanide dihydrate was dissolved in 100 mL of DI water.

2. Preparation of ammonia standard solution

(1) 10.05 mg of NH_4Cl was added into 1000 mL of 0.05 M H_2SO_4 to obtain mother liquor (10 μgNH_3/mL);

(2) 0.4 mL, 0.8 mL, 1.2 mL, 1.6 mL, and 2 mL of mother liquor were separately added into a 20 mL volumetric flask, making up to the mark with 0.05 M H_2SO_4 to obtain 0.2 μgNH_3/mL, 0.4 μgNH_3/mL, 0.6 μgNH_3/mL, 0.8 μgNH_3/mL, 1.0 μgNH_3/mL standard solutions.

3. Determination of ammonia standard curve

(1) Pipetting 2 ml of the standard solutions into serum bottle.

(2) 2 ml of chromogenic reagent, 1 ml of oxidizing solution, 0.2 ml of catalysing reagent was added to the serum bottle in turn, and allowing the mixture to stand for 2 h for color development.

(3) 2.6 mL of the mixture was added to colorimeter tube from the serum bottle. The absorption spectrum was measured using a UV-vis spectrophotometer ranging from

500 nm~800 nm. The concentration of indophenol blue was determined using the absorbance at a wavelength of 655 nm. Thus, a linear curve of the relationship between ammonia concentration and absorbance can be obtained.

Quantification of Hydrazine:

1. Preparation of hydrazine chromogenic agent.

The hydrazine product in the electrolytes was estimated by the method of Watt and Chrisp. 6.05 g of para-(dimethylamino)benzaldehyde, 30 mL of concentrated hydrochloric acid, and 300 mL of absolute ethyl alcohol were added in a 500 mL volumetric flask as the hydrazine chromogenic agent.

2. Preparation of hydrazine standard solution

(1) 19 μL of hydrazine hydrate was added in 1000 mL of 0.05 M H_2SO_4 to obtain mother liquor (10 μgN_2H_4/mL).

(2) 0.4 mL, 0.8 mL, 1.2 mL, 1.6 mL and 2 mL of mother liquor were separately added into a 20 mL volumetric flask, making up to the mark with 0.05 M H_2SO_4 to obtain 0.2 μgN_2H_4/mL, 0.4 μgN_2H_4/mL, 0.6 μgN_2H_4/mL, 0.8 μgN_2H_4/mL, 1.0 μgN_2H_4/mL standard solutions.

3. Determination of hydrazine standard curve

(1) Pipetting 2 ml of the standard solutions and 2 ml of hydrazine chromogenic agent into the serum bottle.

(2) 2 mL of the mixture was added to colorimeter tube from the serum bottle. The absorption spectrum was measured using a UV-vis spectrophotometer ranging from 400 nm ~ 600 nm. The concentration of the resulting solution was determined using the absorbance at a wavelength of 455 nm. Thus, a linear relationship between the hydrazine concentration and absorbance can be obtained.

Quantification of $^{14}NH_4^+$ *via* ^1H NMR: The standard curve is constructed by

measuring a series of NMR resonance peak for the reference solutions with different $(NH_4)_2SO_4$ concentrations (convert to NH_3: 0.5 μg/mL, 1.0 μg/mL, 1.5 μg/mL, 2.0 μg/mL, 2.5 μg/mL) in 0.05 M H_2SO_4 through integrating the ammonia signal appeared at 6.92 ppm, of which a known amount of deuterated dimethyl sulfoxide (DMSO-d6) is used as an internal standard. All analyses are performed with 600-time scans. After electrolysis at -0.3 V *vs.* RHE for 2 h, 10 mL of the electrolyte is taken out and then concentrated to 2 mL by heating at 70 °C. Subsequently, 0.57 mL of the resulting solution is taken out and mixed with 0.03 mL DMSO-d6 for ^{1}H-NMR measurement. (Bruker Advance III 400).

$^{15}N_2$ isotope labeling experiments: $^{15}N_2$ with the 99 atom% ^{15}N (from Newradar, Wuhan) is used to conduct the isotopic labeling experiment in the 0.05 M H_2SO_4 electrolyte. The cell and electrolyte are repeatedly purged with Ar for several times to remove residual N_2 and O_2. The $^{15}N_2$ is introduced into the electrolyte with the injection of ~100 mL every 10 min. After electrolysis at -0.3 V for 2 h, 20 mL of the electrolyte is taken out and then concentrated to 2 mL by heating at 70 °C. Then, 0.57 mL of the resulting solution is taken out and mixed with 0.03 mL of DMSO-d6 for ^{1}H NMR measurement (Bruker Advance III 400).

NO_x detection: NO_x was detected using N-(-1-naphthyl) ethylenediamine dihydrochloride (NED) spectrophotometric method. Briefly, 5 mg NED, 0.5 g sulfanilic acid, and 5 mL acetic acid are dissolved in 80 mL DI H_2O, and then the mixture is diluted to 100 mL by DI water to obtain the chromogenic agent. Subsequently, 1 mL electrolyte is mixed with 4 mL chromogenic agent and left in darkness for 10 min. The absorption spectrum is measured at 550 nm. The concentration–absorbance curves are calibrated using standard sodium nitrite solution with a series of concentrations in 0.05 M H_2SO_4.

NH_3 Yield Rate (YR) and Faradic Efficiency (FE): The NH_3 yield rate is calculated using the following equation: $YR = (C_{NH3} \times V) / (t \times m)$, where C_{NH3} is the detected NH_3 concentration (μg mL^{-1}), V is the volume of electrolyte (mL), t is the reduction

time (h) and m is the catalyst loading amount (mg). The Faradic Efficiency of NH_3 can be obtained as follow: FE = (3 × F × C_{NH3} × V) / (M × Q), where F is the Faraday constant (96485 C mol^{-1}), M is the molar mass of ammonia (17 g mol^{-1}) and Q is the quantity of integral electricity in a certain reduction time (C).

Calculation details: The first-principle calculations were performed within the framework of density functional theory (DFT) using the Vienna Ab Initio Simulation Package (VASP).[5-6] The generalized gradient approximation of Perdew, Burke and Ernzerhof was used to represent the exchange-correlation energy.[7] The projector-augmented wave (PAW) method, with a 450 eV energy cutoff, was used to describe the wave functions of the atomic cores.[8-9] The Brillouin zone was set to 3×3×1 Monkhorst-Pack k-point mesh. To avoid the artificial iteration between adjacent images, a vacuum layer of 15Å was added along the normal direction to the slab. Geometries were optimized until the energy had converged to 1.0×10^{-5} eV per atom and the force converged to 0.01 eV/Å.

The adsorption energy was calculated using the expression as below:

$$E_{ad} = E_{(sp+slab)} - (E_{sp} + E_{slab}) \qquad (1)$$

where E_{sp}, E_{slab} and $E_{(sp+slab)}$ are the total energies for the isolated species, the clean slab and the slab with the adsorbed species, respectively.

The Gibbs free energy (ΔG) was calculated as:

$$\Delta G = \Delta E + \Delta E(\mathrm{ZPE}) - T\Delta S \qquad (2)$$

where ΔE is the reaction energy, ΔE(ZPE) is the zero point energy difference, and ΔS is the entropy difference between the products and the reactants.

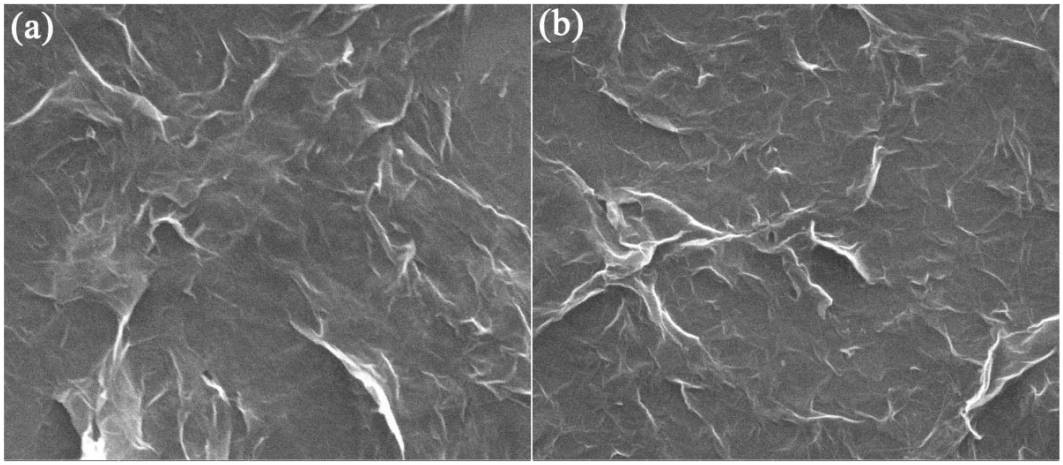

Figure S1. SEM images of (a) RGO and (b) Cl-RGO.

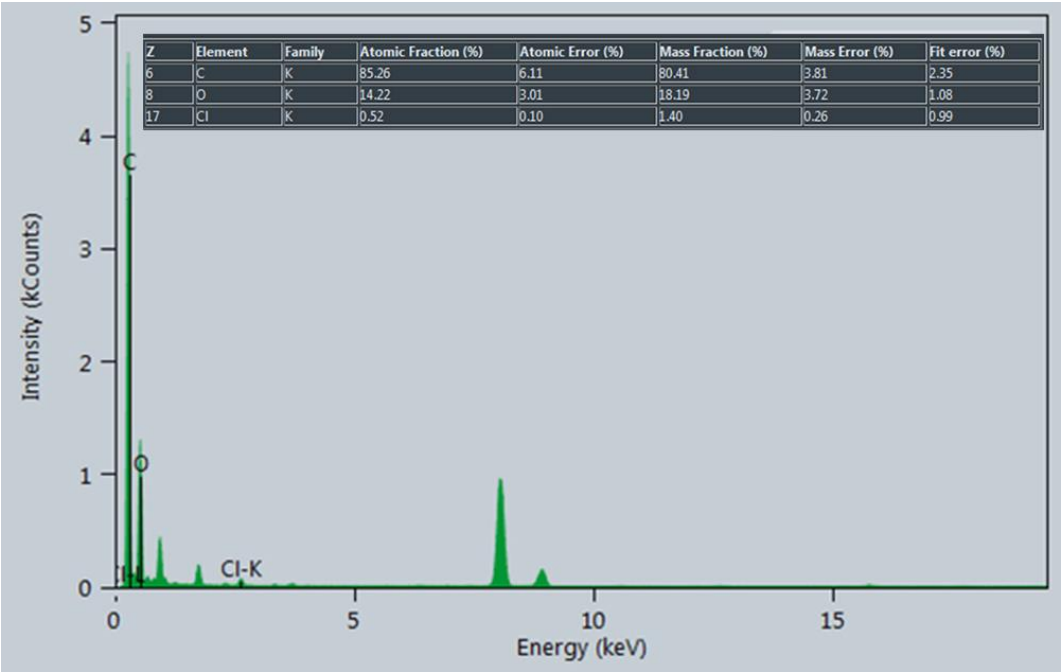

Figure S2. Element content analysis of Cl-RGO by TEM-EDS spectrum.

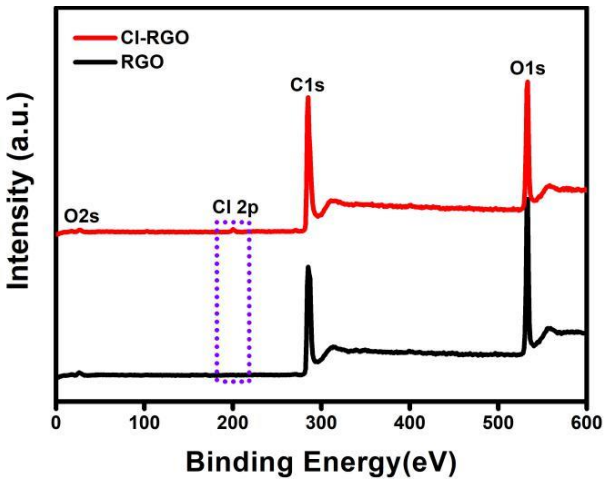

Figure S3. XPS survey spectra for RGO and Cl-RGO. The purple dotted rectangle marks the Cl 2p signals.

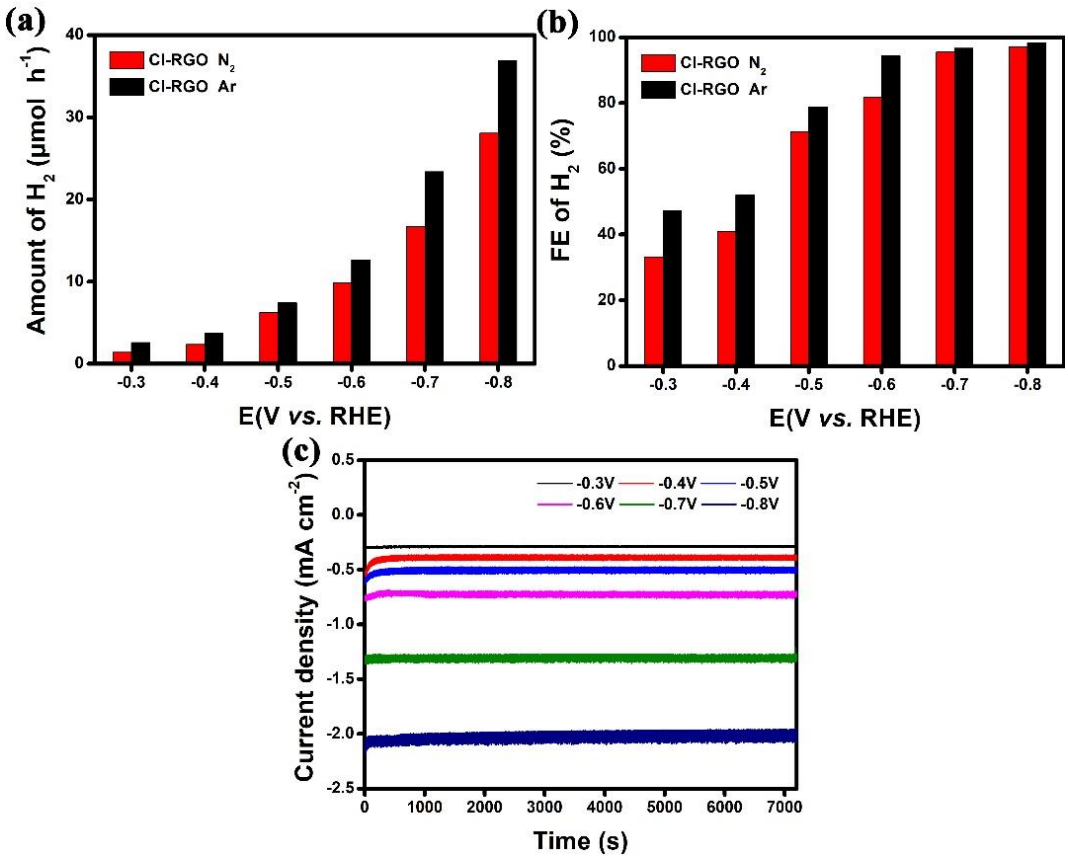

Figure S4. (a) Amount of the evolved H_2 determined by GC in the N_2- or Ar-saturated solutions for Cl-RGO. (b) The corresponding FEs of HER at various potentials. (c) Chronoamperometry tests of Cl-RGO in Ar-saturated 0.05 M H_2SO_4 solutions at various applied potentials. Note: combing the data with the obtained NH_3 selectivity, the missing value can be caused by a combination of factors such as the capacitance of the carbon paper, the dynamic hydrogen adsorption on the catalyst, and the uncontrollable experimental error.

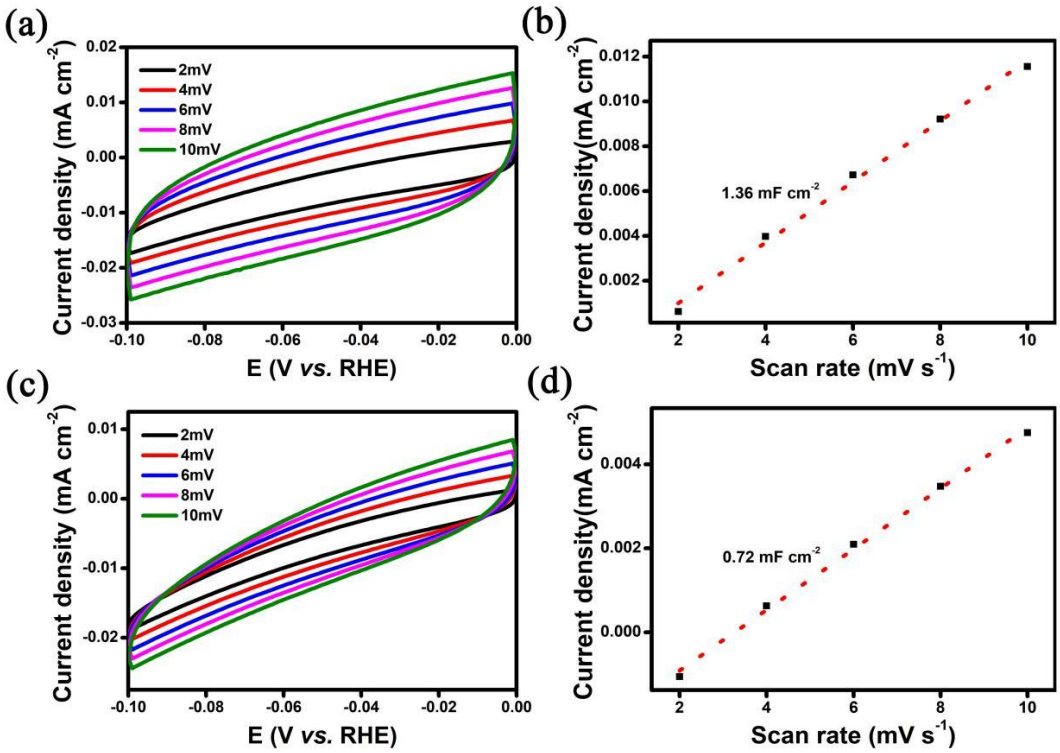

Figure S5. Measured cyclic voltammetry curves on (a) RGO and (c) Cl-RGO with a potential range from -0.10 V to 0 V. The double layer capacitances (C_{dl}) comparison of (b) RGO and (d) Cl-RGO. C_{dl} were obtained from the current density responses at -0.02 V against scan rates.

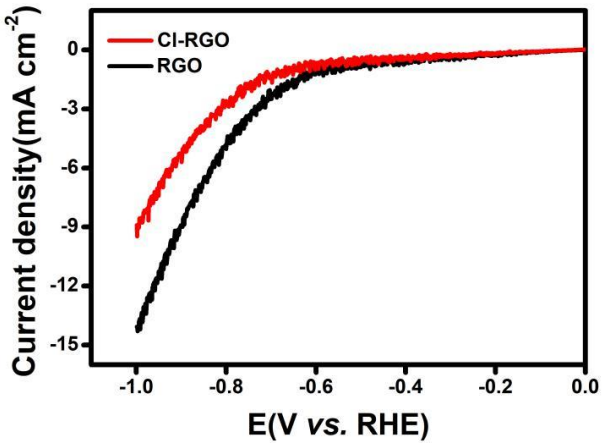

Figure S6. LSV curves of RGO and Cl-RGO in the Ar-saturated 0.05 M H_2SO_4 solution.

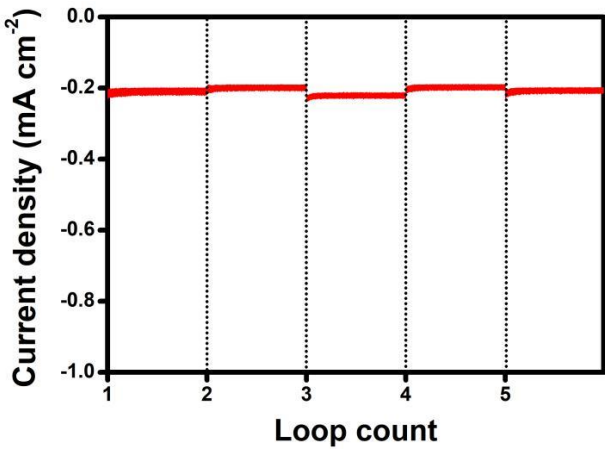

Figure S7. The i-t curves of five runs of 2 h NRR reaction over Cl-RGO at -0.3 V *vs.* RHE.

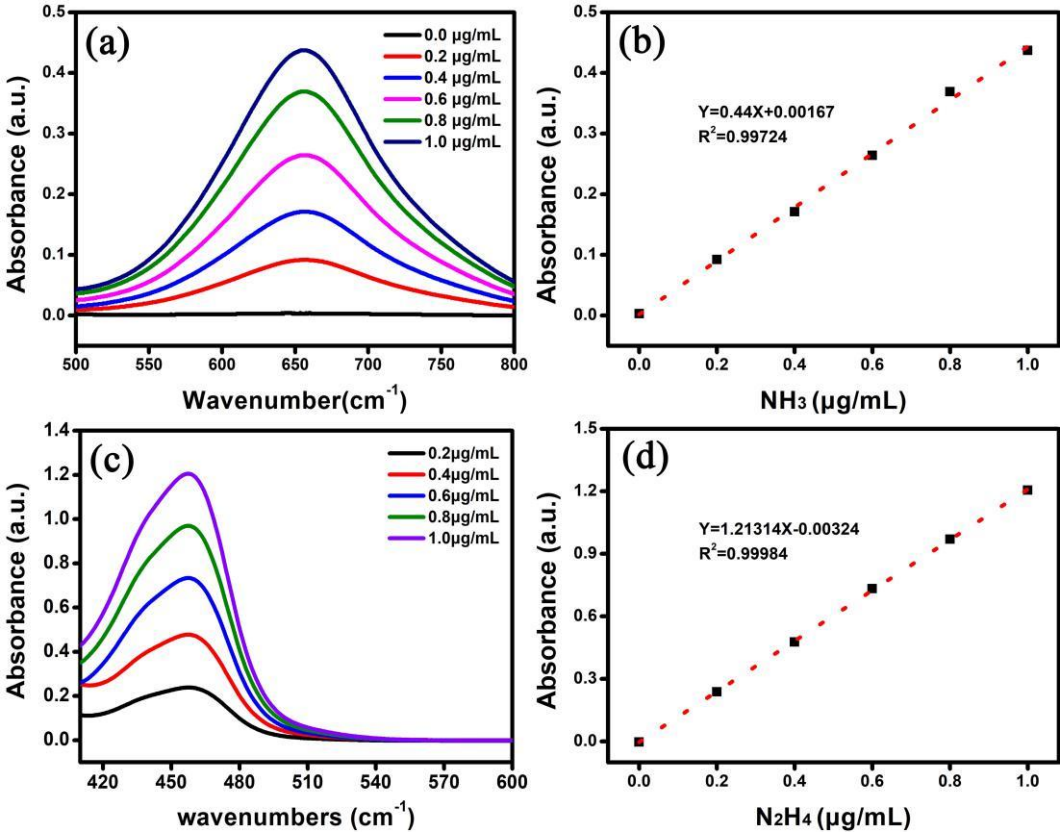

Figure S8. (a) UV-Vis absorption spectra of indophenol assays at different NH_3 concentrations incubated for 2 h and (b) calibration curve used for calculation of NH_3 concentrations. (c) UV-Vis absorption spectra of different N_2H_4 concentrations after incubated for 20 min stained with p-$C_9H_{11}NO$ indicator and (d) calibration curve used for calculation of N_2H_4 concentrations.

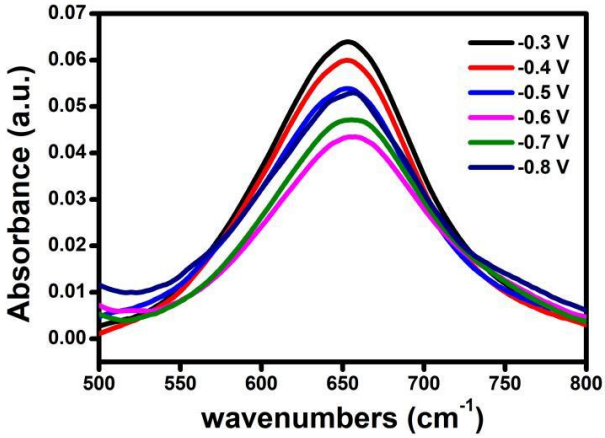

Figure S9. UV-vis spectra of electrolytes stained with indophenol indicator for Cl-RGO at various applied potentials.

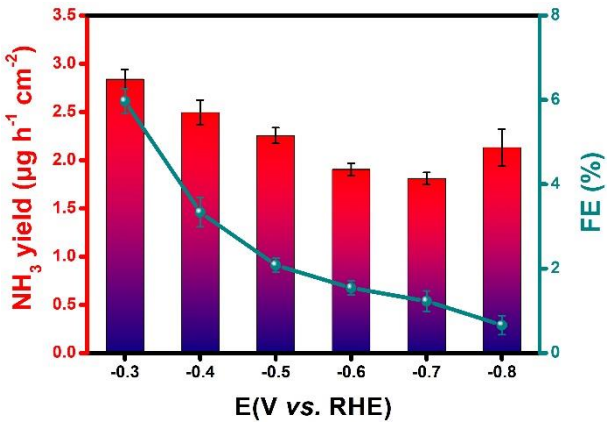

Figure S10. The NH_3 yield (left y-axis) normalized to the geometric surface area of the carbon paper on which Cl-RGO was loaded and the corresponding Faraday efficiency (right y-axis) at various applied potentials.

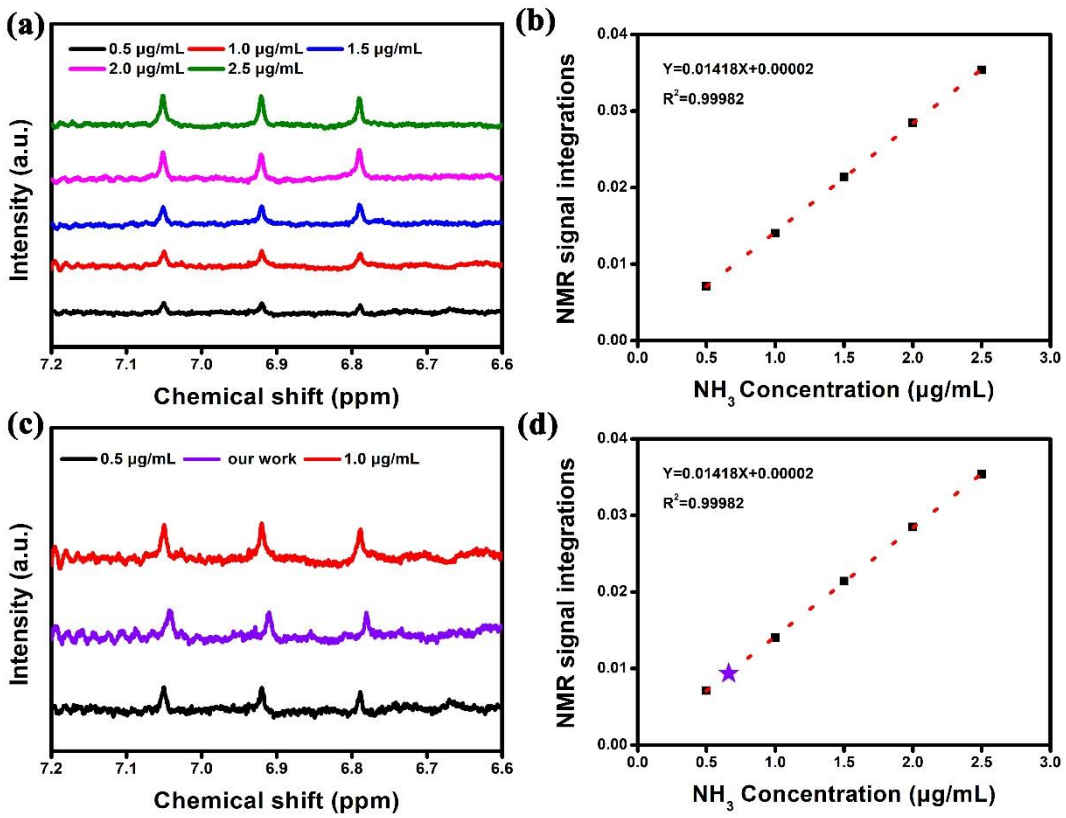

Figure S11. (a) ^{1}H NMR spectra of various $^{14}NH_3$ concentration. (b) Signal integral area ($^{14}NH_3$ / DMSO-d6) against $^{14}NH_3$ concentration. (c) ^{1}H NMR spectra of the electrolyte and the reference solution. (d) The $^{14}NH_3$ concentration of the electrolyte that was quantitatively determined by ^{1}H NMR with external standards.

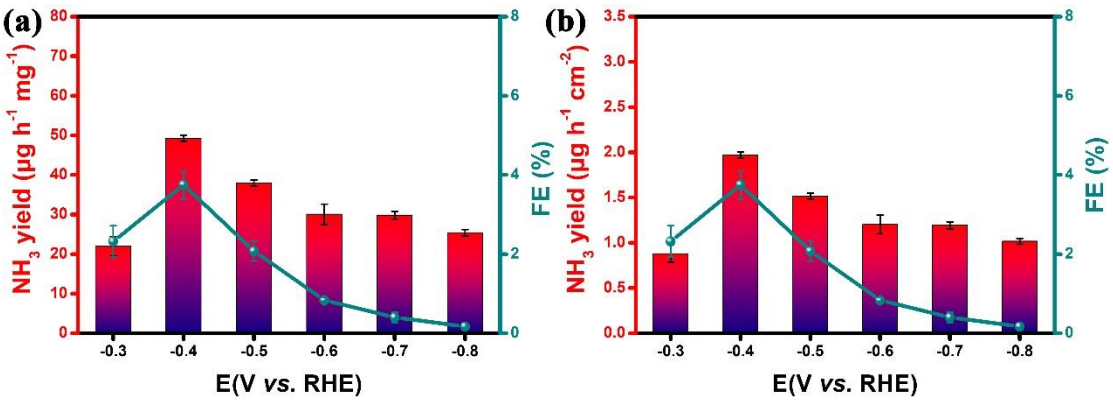

Figure S12. The NH_3 yield (left y-axis) normalized to the mass of the catalyst (a), normalized to the geometric surface area of the carbon paper on which the Cl-RGO catalyst was spread (b), and the corresponding Faraday efficiency (right y-axis) at various applied potentials when Cl-RGO with a lower content of doped Cl (~0.36 atom%) was used as the catalyst.

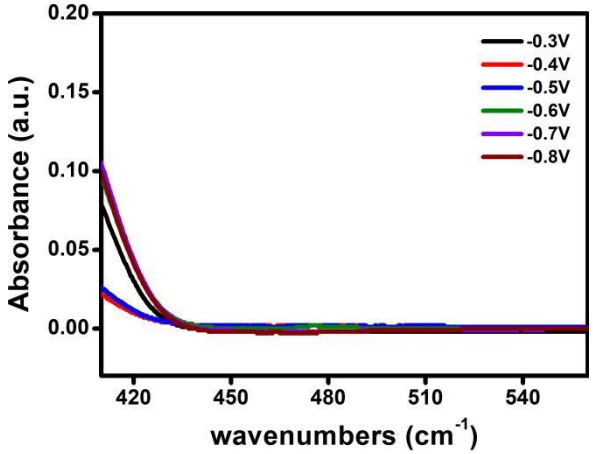

Figure S13. UV-Vis absorption spectra of the electrolytes stained with p-$C_9H_{11}NO$ indicator for Cl-RGO at various applied potentials.

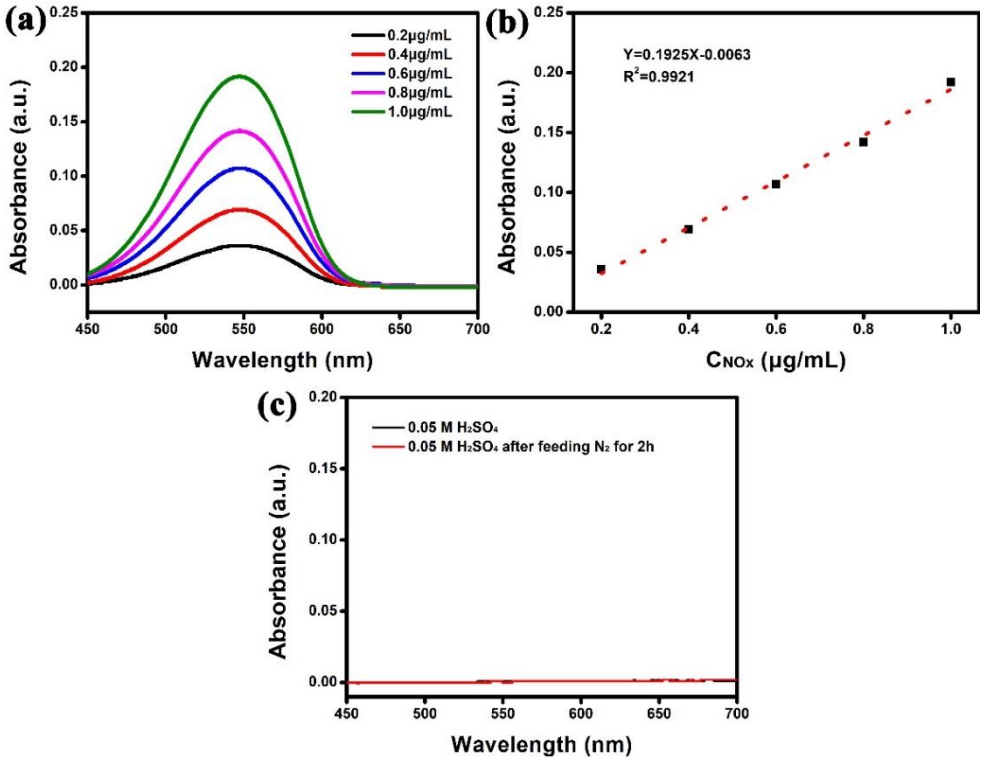

Figure S14. (a) The UV-vis absorption spectra and (b) corresponding calibration curves for the colorimetric NO_x using the NED spectrophotometric method in 0.05 M H_2SO_4. (c) The UV-vis absorption spectra of the blank 0.05 M H_2SO_4 and the N_2 saturated 0.05 M H_2SO_4 solution.

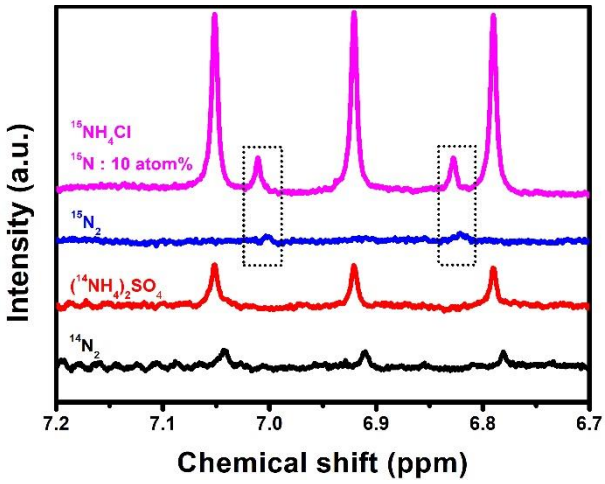

Figure S15. ^{1}H NMR spectra of $^{14}NH_4^+$ and $^{15}NH_4^+$ generated from $^{14}N_2$ and $^{15}N_2$ electroreduction, respectively.

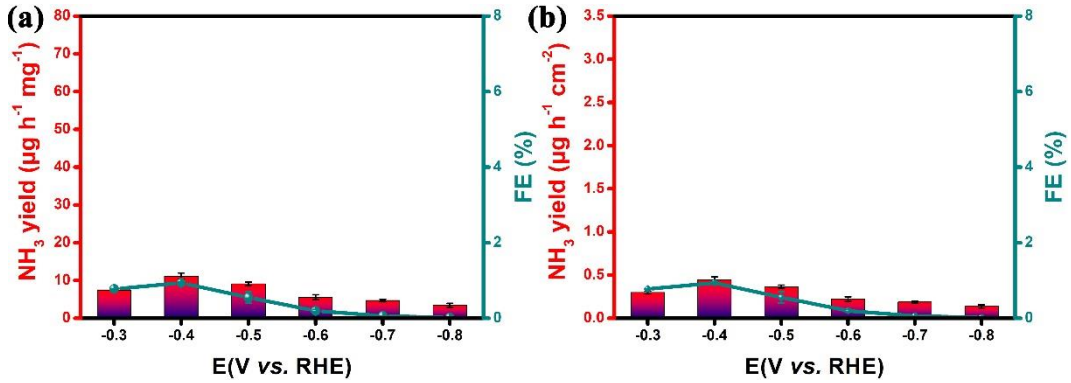

Figure S16. The NH_3 yield (left y-axis) normalized to the mass of the catalyst (a), normalized to the geometric surface area of the carbon paper on which the undoped RGO was spread (b), and the corresponding Faraday efficiency (right y-axis) at various applied potentials when the undoped RGO was used as the catalyst.

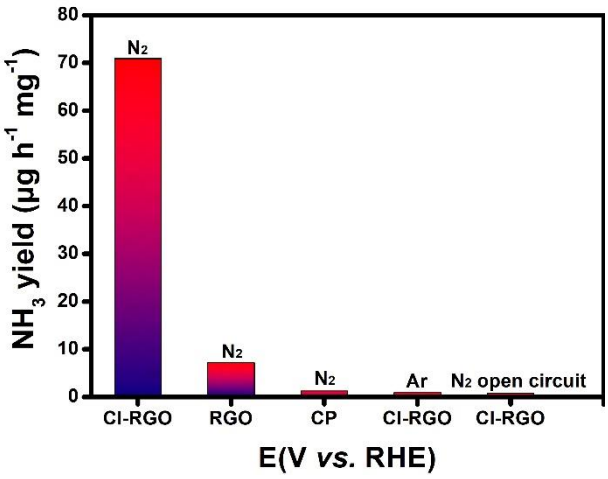

Figure S17. NH_3 yields on different electrodes at the potential of -0.3 V.

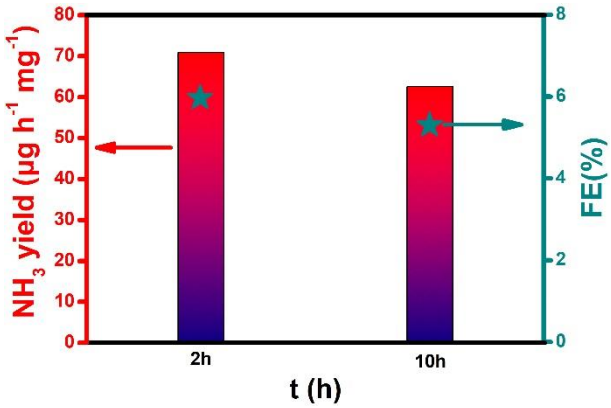

Figure S18. The NRR stability test of Cl-RGO at -0.3 V in the 0.05 M H_2SO_4 solution.

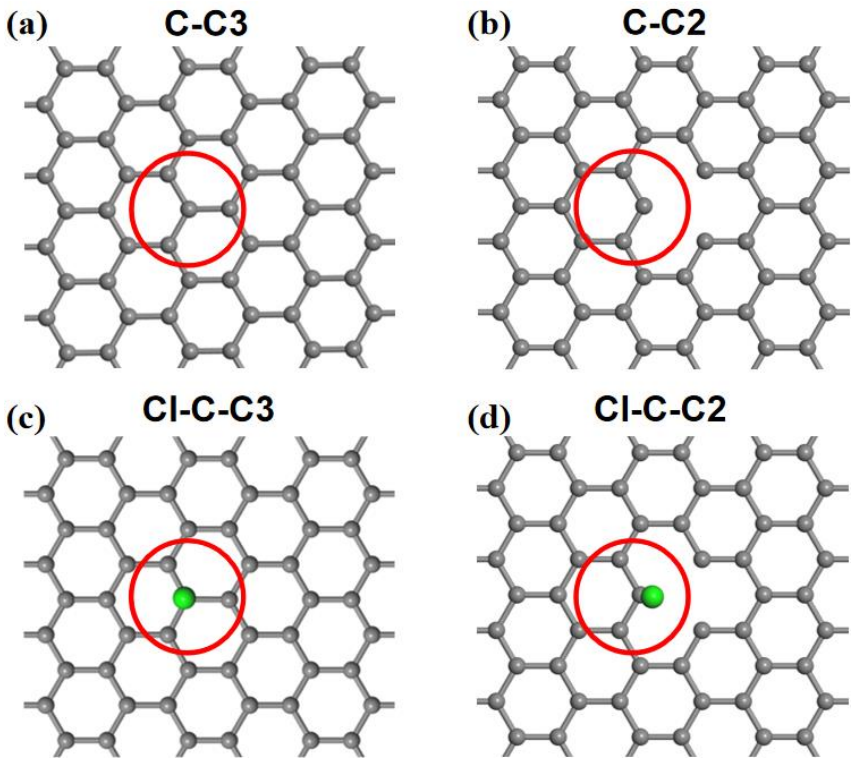

Figure S19. Slab models of RGO with or without Cl dopant, including (a) C-C3 type, (b) C-C2 type, (c) Cl-C-C3 type, and (d) Cl-C-C2 type.

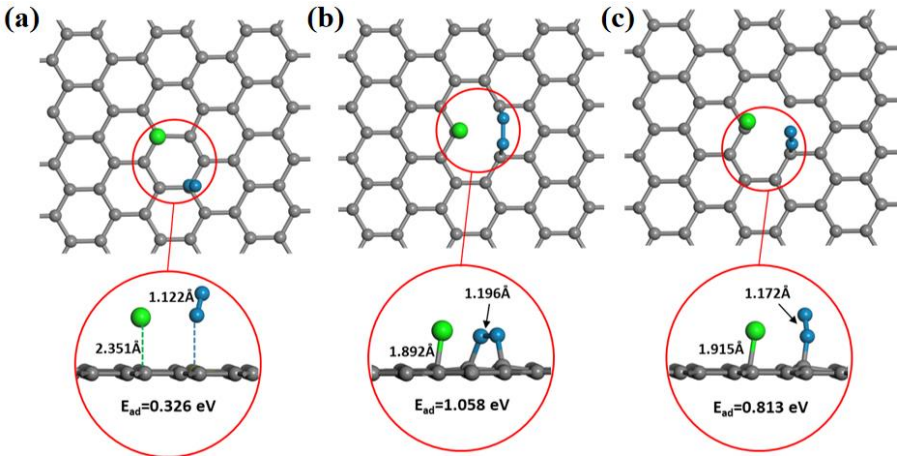

Figure S20. Optimized geometric structures of N_2 adsorption on (a) the C-C3 slab, (b) the Cl-C-C2 slab by the side-on pattern, and (c) the Cl-C-C2 slab by the end-on pattern. The corresponding adsorption energies are given (in eV). Green, grey and blue spheres represent Cl, C and N atoms, respectively.

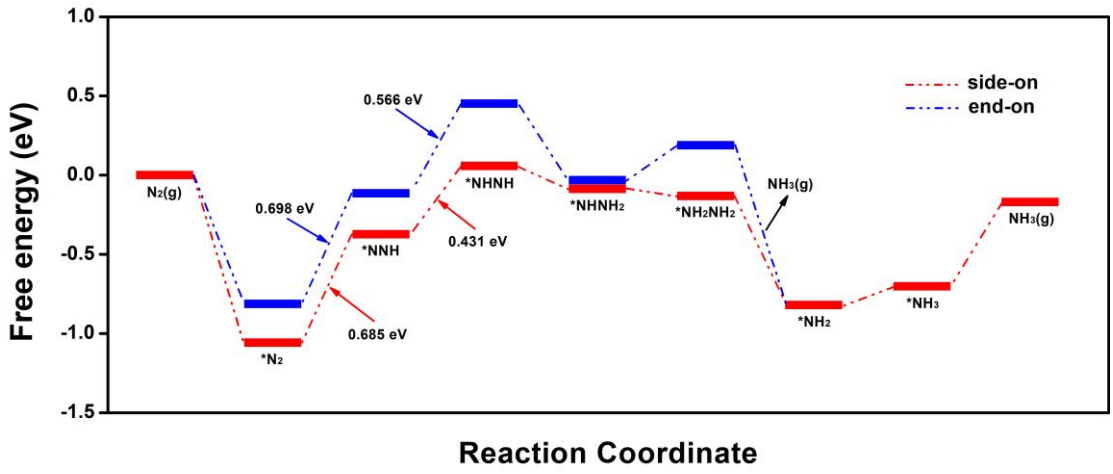

Figure S21. Free energy diagram for the associative alternating pathway during NRR on Cl-C-C2 with adsorbed N_2 in the end-on pattern (red) and in the side-on pattern (blue).

Catalyst	Electrolyte	Yield Rate ($\mu g\ h^{-1} mgcat^{-1}$)	FE (%)	Potential (V vs.RHE)	Ref.
Cl-RGO	0.05 M H_2SO_4	70.9	5.97	-0.3	This work
Boron-doped Graphene	0.05 M H_2SO_4	54.88	10.8	-0.5	[35]
Oxidized carbon nanotubes	0.1 M $LiClO_4$	32.33	12.5	-0.4	[36]
Fluorographene nanosheet	0.1 M Na_2SO_4	9.3	4.2	-0.7	[37]
Fluorine-doped carbon	0.05 M H_2SO_4	16.2	12.1	-0.55	[38]
N-doped porous carbon	0.05 M H_2SO_4	23.8	1.42	-0.9	[S10]
Nitrogen-doped porous carbon	0.1 M HCl	15.7	1.45	-0.2	[S11]
Polymeric carbon nitride	0.1 M HCl	8.09	11.59	-0.2	[S12]
B-N enriched C-carbon	0.1 M HCl	7.75	13.79	-0.3	[S13]
S dots-graphene	0.5 M $LiClO_4$	28.56	7.07	-0.85	[S14]
S-doped carbon	0.1 M Na_2SO_4	19.07	7.47	-0.7	[S15]

Table S1. A comparison of the reported metal-free carbonaceous electrocatalysts for NRR under ambient conditions.

Supplemental References

S1. Wu, K. H.; Wang, D. W.; Zeng, Q.; Li, Y.; Gentle, I. R. Solution Phase Synthesis of Halogenated Graphene and The Electrocatalytic Activity for Oxygen Reduction Reaction. Chin. J. Catal. **2014**, *35(6)*, 884-890.

S2. Kakaei, K.; Hamidi, M.; Husseindoost, S. Chlorine-Doped Reduced Graphene Oxide Nanosheets as An Efficient and Stable Electrode For Supercapacitor In Acidic Medium. J. Colloid Interface Sci. **2016**, 479, 121-126.

S2. Kakaei, K.; Balavandi, A. Synthesis of Halogen-Doped Reduced Graphene Oxide Nanosheets as Highly Efficient Metal-free Electrocatalyst for Oxygen Reduction Reaction. J. Colloid Interface Sci. **2016**, 463, 46-54.

S4. Poh, H. L.; Šimek, P.; Sofer, Z.; Pumera, M. Halogenation of Graphene With Chlorine, Bromine, or Iodine by Exfoliation in A Halogen Atmosphere. *Chem. Eur. J.* **2013**, *19(8)*, 2655-2662.

S5. Kresse, G.; Furthmüller, J. Efficiency of Ab-Initio Total Energy Calculations for Metals and Semiconductors Using a Plane-Wave Basis Set. *J. Comput. Mater. Sci.* **1996**, *6*, 15-50.

S6. Kresse, G.; Furthmüller, J. Efficient Iterative Schemes for Ab Initio Total-Energy Calculations Using a Plane-Wave Basis Set. *Phys. Rev. B.* **1996**, *54*, 11169.

S7. Perdew, J. P.; Burke, K.; Ernzerhof, M. Generalized Gradient Approximation Made Simple. *Phys. Rev. Lett.* **1996**, *77*, 3865.

S8. Blöchl, P. E. Projector Augmented-Wave Method. *Phys. Rev. B.* **1994**, *50*, 17953.

S9. Kresse G.; Joubert, D. From Ultrasoft Pseudopotentials to the Projector Augmented-Wave Method. *Phys. Rev. B.* **1999**, *59*, 1758-1775.

S10. Liu, Y.; Su, Y.; Quan, X.; Fan, X.; Chen, S.; Yu, H.; Zhao, J. Facile Ammonia Synthesis from Electrocatalytic N_2 Reduction under Ambient Conditions on N-Doped Porous Carbon. *ACS Catal.* **2018**, *8*, 1186-1191.

S11. Yang, X.; Li, K.; Cheng, D.; Pang, W. L.; Lv, J.; Chen, X.; Li, Y. G. Nitrogen-Doped Porous Carbon: Highly Efficient Trifunctional Electrocatalyst for Oxygen Reversible Catalysis and Nitrogen Reduction Reaction. *J. Mater. Chem. A.* **2018**, *6*,

7762-7769.

S12. Lv, C.; Qian, Y.; Yan, C.; Ding, Y.; Liu, Y.; Chen, G.; Yu, G. Defect Engineering Metal-Free Polymeric Carbon Nitride Electrocatalyst for Effective Nitrogen Fixation under Ambient Conditions. *Angew. Chem. Int. Ed.* **2018**, *57*, 10246-10250.

S13. Chen, C.; Yan, D.; Wang, Y.; Zhou, Y.; Zou, Y.; Li, Y.; Wang, S. B-N Pairs Enriched Defective Carbon Nanosheets for Ammonia Synthesis with High Efficiency. *Small* **2019**, *15*, 1805029.

S14. Chen, H.; Zhu, X.; Huang, H.; Wang, H.; Wang, T.; Zhao, R.; Sun, X. Sulfur Dots-Graphene Nanohybrid: A Metal-Free Electrocatalyst for Efficient N_2-to-NH_3 Fixation under Ambient Conditions. *Chem. Commun.* **2019**, *55*, 3152-3155.

S15. Xia, L.; Wu, X.; Wang, Y.; Niu, Z.; Liu, Q.; Li, T.; Sun, X. S-Doped Carbon Nanospheres: An Efficient Electrocatalyst toward Artificial N_2 Fixation to NH_3. *Small Methods.* **2019**, *3*, 1800251.